Computational and Theoretical Chemistry 1250 (2025) 115271

Contents lists available at ScienceDirect

Computational and Theoretical Chemistry

journal homepage: www.elsevier.com/locate/comptc

Uptake of Eu(III) by C-S-H phases in $CaCl_2$ solution in presence of EDTA: A molecular dynamics study

Iuliia Androniuk *, Aline K. Thumm, Andrej Skerencak-Frech, Marcus Altmaier, Xavier Gaona

Institute for Nuclear Waste Disposal (INE), Karlsruhe Institute of Technology (KIT), Karlsruhe, Germany

ARTICLE INFO

Keywords:
C-S-H
Europium(III)
EDTA
Ternary complexes
Molecular dynamics
Sorption

ABSTRACT

The presence of organic ligands in radioactive waste influences radionuclide mobility and sorption in cement. Although EDTA is often assumed to have minimal impact, recent experiments indicate reduced Eu(III)/Cm(III) uptake by calcium silicate hydrate (C-S-H) at high EDTA concentrations in $CaCl_2$ solutions. We used molecular dynamics (MD) simulations and potential of mean force calculations to investigate complexation and sorption mechanisms. Focusing on the (001) surface of C-S-H, we analyzed radionuclide behavior in the presence of organic ligands under repository-relevant conditions. Solution-phase simulations identified three probable Eu/EDTA/Ca complexes. Sorption at two common sites was examined. Site-specific analysis shows that Ca–Eu(III)–EDTA complexes remain stable in solution, significantly reducing Eu(III) uptake by C-S-H. These findings align with experiments and highlight the role of ternary complex formation in limiting radionuclide retention in cementitious environments.

1. Introduction

Cement plays a critical role in the construction and safety prediction of radioactive waste repositories due to its structural functionality and high radionuclide retention capabilities, making it a key component in multi-barrier systems designed to prevent radionuclide release into the environment [1,2,3,4]. The calcium silicate hydrate (C-S-H) phases, the main binding phases in cement, contribute to both its strength and its ability to adsorb metal ions, including actinides and lanthanides. In deep geological repositories, cement is used not only for structural purposes, but also as a barrier within the packaging and sealing of waste, providing a stable, high-pH environment that enhances radionuclide retention.

Understanding sorption mechanisms at the molecular level is essential for predicting migration in geological disposal systems. This study focuses on accurately modeling the interaction of Eu(III) with C-S-H phases to analyze radionuclide retention and migration under repository-relevant conditions. The molecular modeling of C-S-H – using defect tobermorite as an analogous solid phase structure – requires large simulation cells and extensive computation, which are necessary for achieving accurate representations of C-S-H interactions with radionuclides [5,6]. This computational approach helps to interpret the sorption dynamics within near- and far-field environments, contributing to process understanding and thus improving confidence in the quantitative description of retention phenomena. The C-S-H surface model was built from the initial structure of tobermorite 14 Å ($Ca_5Si_6O_{16}(OH)_2{\cdot}7H_2O$) [7] as it is the closest known crystal structure to real cement phase [8,9,10]. The structure is composed of sheets of seven-fold coordinated calcium cations with silicate chains on both sides. The interlayer space contains additional calcium cations and water molecules.

Eu(III) was selected as a representative model for trivalent actinides and lanthanides (e.g. Am(III), Pu(III)) commonly expected in nuclear waste. It shares a similar charge-to-size (z/d) ratio, coordination chemistry, and complexation behavior with both organic and inorganic ligands. The presence of organic ligands can increase the mobility of radionuclides by enhancing their solubility or decreasing sorption due to (i) the formation of stable complexes in the aqueous phases or (ii) competition for the sorption sites at cementitious or mineral interfaces [11,12].

Molecular dynamics simulations have significantly advanced our understanding the hydration structure of europium(III) and its interactions with organic ligands. Numerous computational studies have examined the hydration shell of Eu(III), using a range of methods with varying levels of accuracy [13,14,15]. For example, Clavaguéra et al. [16] introduced many-body effects into their models to better capture

* Corresponding author.
E-mail address: iuliia.androniuk@partner.kit.edu (I. Androniuk).

https://doi.org/10.1016/j.comptc.2025.115271
Received 18 February 2025; Received in revised form 24 April 2025; Accepted 29 April 2025
Available online 29 April 2025

the structure of the solvation shell and the water exchange dynamics of trivalent lanthanides, achieving better agreement with experimental results. However, increased model accuracy often comes at the cost of computational efficiency, making it necessary to achieve a balance between precision and feasibility.

Several studies have also focused on the binding of Eu(III) to different organic ligands, e.g. diglycolamide [17], dipicolinate [18], and BTP-based ligands [19]. To facilitate such simulations, Veggel and Reinhoudt [20] proposed a set of Lennard-Jones (LJ) parameters for Eu (III) that are compatible with organic force fields and produce results that are in good agreement with experimental observations [18,19]. These parameters were adopted in our study to ensure both reliability and computational efficiency.

Ethylenediaminetetraacetic acid (EDTA) is a common decontamination agent and is expected in some waste streams in the disposal of low and intermediate level waste (L/ILW). EDTA has six functional groups (four carboxyl and two amine), and is known for its strong chelating properties, which allow it to effectively bind and remove polyvalent metal ions, including radionuclides, from surfaces and solutions. EDTA is generally thought to have a minimal impact on radionuclide retention in cement-based environments because it strongly complexes with calcium, which is present at concentrations significantly higher than radionuclides. Multiple studies have confirmed that at low concentrations ($<10^{-3}$ M) there is no significant effect of the presence of EDTA presence on the sorption of Eu(III) in C-S-H and hydrated cement paste [21,22,23,24].

However, the latest results obtained from batch sorption and TRLFS (time-resolved laser-induced fluorescence spectroscopy) experiments have shown that there is a considerable decrease in Eu(III) uptake by the C-S-H phases (Ca/Si = 0.7–1.3) in the presence of EDTA with concentrations higher than 10^{-3} M in $CaCl_2$ solutions, or in NaCl solutions for C-S-H phases with Ca/Si $\geq$ 1.3 [24]. The latter system is also characterized by higher aqueous calcium concentrations compared to C-S-H 0.7 and 1.0. It was concluded that the presence of sufficiently high Ca concentrations in solution triggers the formation of stable ternary Ca–Eu (III)–EDTA species, which stabilize Eu(III) in solution and minimize its sorption. An analogous effect was described by Dario and co-workers for the uptake of Eu(III) by cement at EDTA concentrations above 10^{-3} M [22]. Additionally, similar observations have been reported for Ca/Eu (III)/gluconate and Ca/Pu(IV)/isosaccharinate systems [25,26,27].

The Eu/EDTA complexes in our work are studied as preformed *endo* complexes, where the cation already coordinates monodentately the four carboxylate groups and the two N atoms of the ligand. This decision was made because the spontaneous formation of the *endo* complexes cannot be modeled with classical molecular dynamics simulations [28]. Several studies suggest that, in the absence of Ca, Eu(III) may form ternary complexes Eu(III)–OH–EDTA at pH values higher than 9 [29,30]. In the presence of Ca, DiBlasi and co-workers hypothesized the formation of quaternary complexes Ca-Pu(III)/Cm(III)-OH-EDTA only above pH 12, whilst below this pH the formation of ternary complexes Ca-Pu(III)/Cm(III)-EDTA was suggested. Using a combination of EXAFS and MD simulations, the recent work by Licup et al. [31] hinted that water molecules remain in the first coordination sphere of Eu(III) even at pH 11. In the modeled experiment of Thumm et al. [24] at pH 11.5, the presence of hydroxyl groups in the first coordination sphere could not be conclusively demonstrated. With this background, the coordination of Eu(III) with aqueous hydroxyls in the presence of EDTA was not considered in our model, although we acknowledge that they may form (even in the presence of Ca) in a more alkaline pH-regime.

The formation of aqueous systems at elevated ionic strength conditions needs to be considered for underground repositories in rock salt formations, but also for other potential host rock formations located in the vicinity of rock salt layers. Such conditions are found, e.g. in northern German clay rock formations, where the clay pore water shows a very high salinity of up to 5 M (mostly defined by sodium chloride, with magnesium or calcium as additional cations) [32]. It is important to understand and describe the sorption sites and local complex structures of Eu(III) adsorbed on the C-S-H surface in the presence of EDTA and Ca. Therefore, we developed this computational modeling study to interpret the macroscopic experimental data and identify molecular mechanisms undelying the sorption and desorption phenomena.

2. Computational methods

To study the behavior of the Eu(III)/EDTA complex in a concentrated $CaCl_2$ solution, an orthogonal simulation box was built with dimensions of 50 Å × 50 Å × 50 Å, which contained 4096 water molecules with 2 $EDTA^{4-}$, 2 Eu/$EDTA^{-}$ complexes, 29 Ca^{2+}, and 48 Cl^{-} ions randomly distributed. This approximately corresponds to 0.33 M $CaCl_2$ and 0.01 M EDTA ion concentration. The total electroneutrality of the simulation cell was ensured by balancing the number of counterions. Periodic boundary conditions were applied in three dimensions. The model system was initially equilibrated for 5 ns in the isobaric−isothermal statistical ensemble (*NPT*) and subsequently for 5 ns in the canonical ensemble (*NVT*). Temperature and pressure were constrained using the Nose−Hoover thermostat and barostat under ambient conditions (T = 295 K, a room temperature, P = 0.1 MPa). Production run was recorded during 10 ns in the *NVT* ensemble. Radial distribution functions (*g(r)*) and running coordination numbers (*n(r)*) for Eu–X atom pairs (where X represents atom types present in the simulation cell) were computed to analyze the local structure of the Eu/EDTA complexes:

$$g_{EuX}(r_{EuX}) = \frac{\overline{N}_{EuX}}{4\pi\rho_X r_{EuX}} \quad (1)$$

$$n_{EuX} = 4\pi\rho_X \int_0^{r_{EuX}} g_{EuX}(r) r^2 dr \quad (2)$$

where $\overline{N}_{EuX}$ is the average number of X atoms at a distance r_{EuX} from the Eu atom, ρ_X is the number density of X atoms (i.e., the number of X atoms per unit volume).

To build the C-S-H surface, the crystallographic unit cell of tobermorite was multiplied (8 × 8 × 2) to create a relatively large simulation supercell to accumulate better statistical data. The simulation cell was then cleaved in the middle of the interlayer along the (001) crystallographic plane to form a surface. Next, defects and adjustments were made to the cleaved surface to create a C-S-H model typical for a Ca/Si ratio of 1.4, with initial dimensions of 54 × 54 × 100 $Å^3$ (a triclinic cell with $\alpha = \beta = 90°$, and $\gamma = 66.5°$, including a vacuum gap). Experimental studies on C-S-H phases with a high Ca/Si ratio (>1.4) show that the mean chain length in the silicate layer is expected to be around 2.3, so the bridging Si tetrahedra were randomly deleted according to available experimental NMR and IR data [33,34,35], and additional Ca^{2+} and OH^{-} ions were introduced. The silanol groups of the bridging Si and one of the pairing Si were deprotonated based on the expected protonation state of the surface at high pH [36]. The deprotonated oxygens on the surface were assigned a partial charge of $q_{onb} = 1.3|e|$, higher than the protonated ones in the standard ClayFF force field [37,38]. The extended gap between the cleaved surfaces was filled with solution molecules. The charge of the total simulation cell was neutral.

The interaction parameters for the surface were taken from the ClayFF force field, known for their reliability and accuracy in cement/water interface simulations [39,40,41]. For the EDTA molecule, parameters were taken from the General Amber force field (GAFF; [42]). Water was modeled using the extended simple point charge (SPC/E) model [43]. Parameters for Eu(III), which have been proven to be compatible with the organic force fields, were taken from [20].

Standard Lorentz−Berthelot mixing rules were applied to calculate short-range Lennard-Jones interactions between unlike atoms, using a cut-off distance of 14 Å. Long-range electrostatic forces were evaluated using the Ewald summation method. All molecular dynamics

simulations were performed using the LAMMPS software package (September 29, 2021 version; [44]). The equilibration of the model system was carefully monitored by evaluating the temperature, pressure, kinetic, and potential energy of the system, and the dimensions of the simulation box, to verify that these parameters reach their equilibrium steady-state values on average, ensuring that the system accurately represented the desired conditions [45].

The C-S-H surface was equilibrated for 5 ns in the *NPT* ensemble together with the $CaCl_2$ solution (26 Ca^{2+}, 47 Cl^-, 5 OH^-) prior to introducing Eu(III) and EDTA (2 *endo* complexes) into the interface solution. The Newtonian equations of the atomic motions were then numerically integrated with a timestep of 1 fs. The model systems were again equilibrated for 5 ns in the *NPT* and *NVT* ensembles each ($T = 295$ K, $P = 0.1$ MPa). To prevent drifting of the modeled systems, four Si atoms from each silicate layer were immobilized during *NVT* production runs, although they were still allowed to interact with other atoms. The VMD software package (version 1.9.3) was used for visualization of simulation trajectories [46].

The potential of mean force (PMF) calculations were used to get insight into the energy landscape of a system, helping to understand the thermodynamics of a process or the stability of different states. In this study, PMF calculations were applied to quantitatively describe the adsorption free energy profiles of the Eu/EDTA complexes as a function of their distance from the C-S-H surface.

The 'umbrella sampling' algorithm was used to sample rarely visited atomic configurations of the system with statistical accuracy that would be unattainable through standard MD simulations [47]. In this technique, biasing potentials are applied to enhance sampling in specific regions. While highly precise, this method is computationally expensive. Therefore, only the two most typical sorption sites for Eu(III) were selected on the (001) surface of C-S-H with high Ca/Si [25]: the bridging site (deprotonated silanol group of the bridging Si), and the defect site (deprotonated silanol groups of pairing Si (see Fig. 1).

A complete PMF calculation involves multiple independent molecular dynamics simulations with biasing potentials applied along the chosen reaction coordinate. For each PMF curve, approximately 100 biased MD simulations were run in the *NVT* ensemble (2 ns each) to cover the entire reaction coordinate. The *z*-distance between the topmost oxygens of the surface and europium was selected as the collective variable. Additional weak *xy* constraints were applied as a 'soft cylindrical wall' of a small diameter to maintain the position of Eu(III) on top of the sorption site.

The umbrella sampling calculations were performed using the COLVARS module integrated into the LAMMPS software package [48]. The weighted histogram analysis method (WHAM) was employed to compute the free energy profiles along the reaction coordinate from the umbrella sampling data. All simulations for each constrained distance window are independent and were run in parallel. The Monte Carlo bootstrapping approach implemented in the WHAM algorithm was used to calculate statistical uncertainties [49,50].

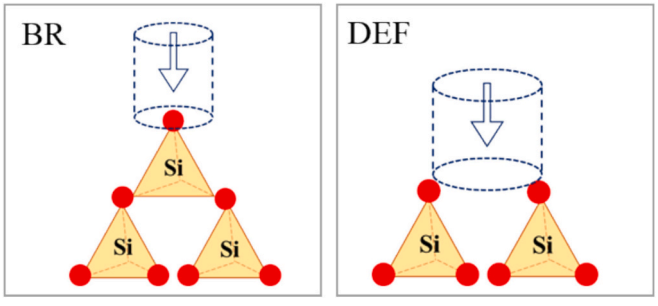

Fig. 1. Schematic representation of the two main sorption sites on the (001) surface of C-S-H with a high Ca/Si ratio: bridging (BR), defect (DEF).

3. Results and discussion

1.1. Interaction of Eu(III)/EDTA complexes with Ca^{2+} in $CaCl_2$ solution.

At high pH conditions characteristic for cement-based systems (pH > 11), EDTA is fully deprotonated, and the structure of its binary complex with Eu(III) (i.e., $Eu(EDTA)^-$) is already well-known. The structure of Eu/EDTA was predicted by classical molecular dynamics studies (Durand et al., 2000; [31]) and validated by extended X-ray absorption fine structure (EXAFS) measurements [51]. They revealed a coordination environment in which the Eu^{3+} ion is bound by four carboxylate groups in a monodentate manner, both amine groups, and three water molecules.

In this work, the behavior of Eu/EDTA complexes in a 0.33 M $CaCl_2$ solution was analyzed to determine the most likely geometries of Ca-containing complexes. The local structures around Eu(III) were examined by calculating the radial distribution functions and corresponding running coordination numbers for atom pairs involving Eu(III) from the 10 ns trajectory. The findings are presented in Figs. 2a (Table SI-1 in Supporting Information) and 2b.

The Eu/EDTA complex was introduced as an *endo* complex into the simulation cell, with analysis confirming that the complex structure remained stable throughout the simulation. A single peak corresponding to the coordination of Eu(III)-carboxyl oxygen (O_{carb}) clearly appears between 2.2 and 2.8 Å, as shown in Fig. 2a. A secondary peak between 4.3 and 4.6 Å indicates the proximity of the second oxygen within each carboxyl group of EDTA. Fig. 2b further reveals that all four carboxylate groups are consistently bound to Eu(III) in a monodentate manner (n $(r)_{Eu\text{-}Ocarb} = 4$ at 2.7 Å and 8 at 4.6 Å). A distinct N peak is found at $d =$ 2.6–3.0 Å and corresponds to the inner sphere binding of two amine groups. The water oxygen peak overlaps with the O_{carb} distance, followed by a hydrogen peak at 3.3 Å, and the calculated running coordination number confirms the presence of three water molecules in the first coordination sphere of Eu(III).

Altogether, in the $CaCl_2$ solution, Eu(III) coordinates with six atoms from a single EDTA molecule: four carboxylate oxygens and two amine groups. This primary coordination shell is completed by three water molecules from the solution, giving Eu(III) a total coordination number of 9. These results align well with the values reported by Licup et al. [31], despite differences in the water model (SPC/E here and TIP3P in Licup et al.). This structure is further validated by both spectroscopic studies [51] and computational studies (O'Brian, 2022).

No major peak is observed for Cl^-, which remains as a background ion in the solution, appearing only at distances greater than 5 Å and showing no participation in the Eu/EDTA/Ca complexation. Additionally, the absence of an Eu—Eu peak confirms that polymerization or precipitation do not occur under these conditions.

The simulation was carried out in a Ca-rich solution ($c = 0.33$ M), where Ca was observed at distances of 3–4 Å from Eu(III), indicating Ca coordination with the carboxyl groups of EDTA molecules. To assess the statistical significance of Ca complexation with Eu/EDTA, the Eu(III) coordination sphere was monitored over a 10 ns production run, categorizing binding configurations into three types: complexes without Ca, complexes with one Ca, and complexes with two Ca. The results indicate that complexes with one Ca formed 75 % of the time, while Eu/EDTA remained uncoordinated or bound to two Ca in 13 % and 12 % of the instances, respectively. Thus, all three configurations were selected for computational sorption studies on the C-S-H surface. In particular, Ca predominantly has monodentate coordination with the deprotonated carboxyl groups of EDTA, as shown in the simulation snapshots in Fig. 3.

Formation of Ca-stabilized Eu/Eu(OH)-EDTA complexes was indirectly hinted by experimental studies on the trivalent lanthanide and actinide ions with EDTA in presence of Ca^{2+}. Batch solubility, time-resolved laser fluorescence spectroscopy (TRLFS) and density functional theory (DFT) studies on Pu(III) and Cm(III) suggested existence of

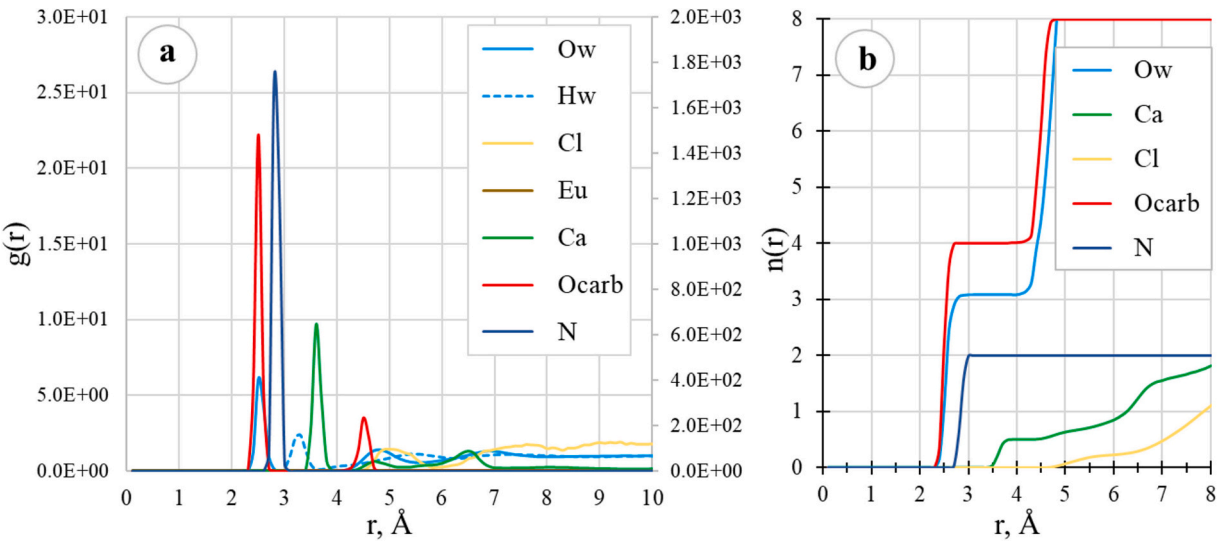

Fig. 2. (a) Radial distribution function for pairs of Eu-X atoms, where X – atom types present in the simulation cell. (b) Corresponding running coordination numbers for selected pairs of Eu-X atoms.

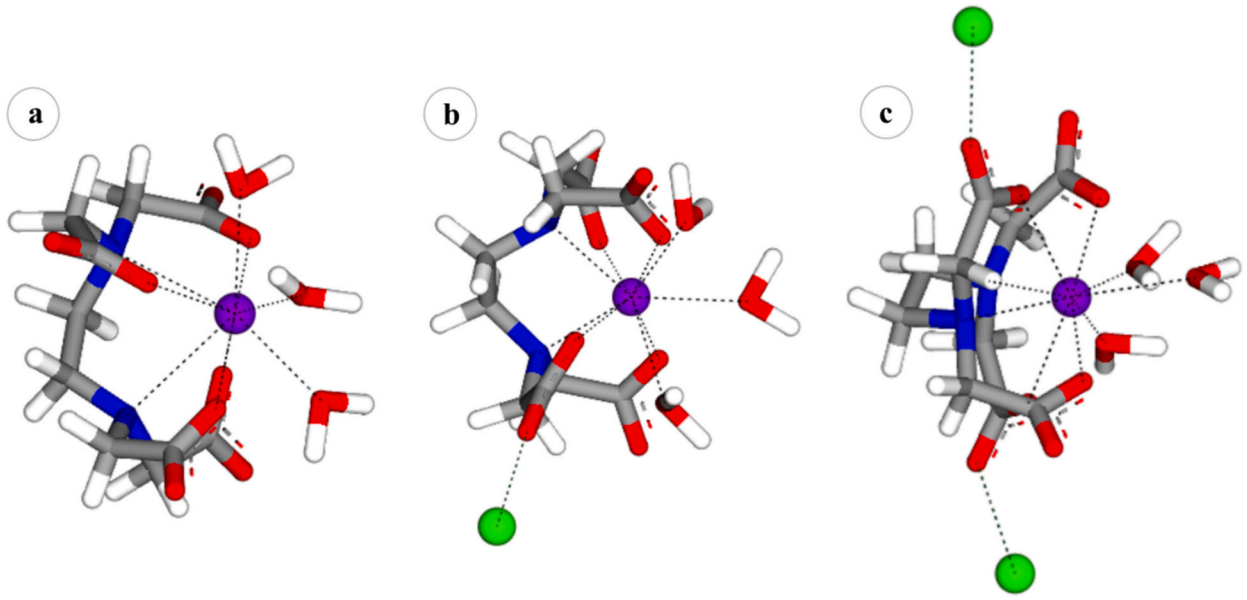

Fig. 3. Simulation snapshots of Eu(III) complexes with EDTA without Ca^{2+} (a), with one Ca^{2+} (b), and with two Ca^{2+}. Colour scheme: Eu – lilac, O – red, C – grey, H – white, N – blue, Ca – green. (For interpretation of the references to colour in this figure legend, the reader is referred to the web version of this article.)

Pu/Cm(III)–OH–EDTA, Ca–Pu/Cm(III)–EDTA, and Ca–Pu/Cm(III)–OH–EDTA complexes in aqueous solutions [30]. Also, the batch sorption and TRLFS study in Thumm et al. [24] showed very stable soluble complexes, tentatively defined as $Eu/Cm(OH)(EDTA)^{2-}$, $Cm(OH)_x(EDTA)^{-(x+1)}$ and Ca–Eu/Cm(III)-EDTA, formed in $CaCl_2$ solution. However, no conclusive evidence on the stoichiometry and structure of such complexes was available to date. For the first time, MD calculations support the formation of the ternary complexes $Ca[Eu(EDTA)]^+$ and (to a lesser extent) $Ca_2[Eu(EDTA)]^{3+}$ in alkaline solutions containing EDTA and Ca. Analogous complexes were previously described for the Ca-Pu (IV)-EDTA system [30], and also for the complexation of Ln(III)/An (III) and An(IV) with other chelating ligands, e.g., (gluconate, isosaccharinate, citrate) [25,52,26,53,54,55,56]. Thus, the assumption that Ca outcompetes radionuclides in the complexation with strong chelating ligands must be carefully assessed for each individual system.

3.1. Sorption of Eu(III)/EDTA/Ca complexes on the (001) surface of C-S-H

3.1.1. Sorption at the bridging sorption site

The uptake of Eu(III) by C-S-H phases and cement has been widely studied using various sorption and spectroscopic techniques. These studies have confirmed that C-S-H plays a primary role in europium retention, with surface sorption and incorporation into the structure identified as the two main uptake mechanisms [57,58,59]. In this study, incorporated species are not considered due to their strong immobilization within the structure, which makes them inaccessible to the solution and, thus, unavailable for interaction with organics at the solid-solution interface.

The potential of mean force curves was calculated to study the sorption of Eu/EDTA complexes with a varying number of Ca at the two most common sorption sites of C-S-H. As a reference for comparison, PMF curves of $Eu(OH)_4^-$ on these sites were taken from our previous

work [25] and plotted together with the new data. In addition, PMF curves for Ca^{2+} sorption were calculated to evaluate possible sorption competition.

All PMF curves for the bridging sorption site are presented in Fig. 4 (Tables SI-2 and SI-4 in Supporting Information). As previously reported in [25], under high pH conditions $Eu(OH)_4^-$ forms a strong inner sphere complex at the bridging sorption site of the (001) surface of C-S-H, with a distinct minimum at $d = 2.3$ Å ($\Delta G_{min} = -34$ kJ/mol). This surface complex can be considered as analogous to the $Ca_x[Ln/An(OH)_4]^{2x-1}$ aqueous complexes described by Neck and co-workers in alkaline $CaCl_2$ solutions [60]. Only weak outer sphere complexes are formed at distances between 4 and 5 Å (ΔG_{min} less than 5 kJ/mol).

The calculated adsorption free energy profile of the Eu/EDTA complex without coordinated Ca^{2+} practically overlaps with the curve for $Eu(OH)_4^-$; the only difference is a higher energy barrier ($\Delta d \approx 10$ kJ/mol) at $d = 2.9$ Å. In the presence of Ca^{2+}, sorption through the inner sphere complexation of Eu/EDTA tends to be weaker: $\Delta G_{min} = -14$ kJ/mol for one Ca^{2+} and − 19 kJ/mol for two Ca^{2+} at $d = 2.3$ Å. At the same time, the energy barrier to form these surface complexes is higher, also considering a more pronounced energy minimum for outer sphere complexation at $d = 4.1$–4.3 Å for both PMF curves.

The complex was free to approach the surface naturally, with only the distance between the Eu(III) and the deprotonated silanol groups controlled and without restrictions on the EDTA molecule. Although it is possible that the Eu/EDTA complex could adsorb by binding EDTA to surface Ca ions or by having EDTA/Ca attach at sorption sites, this behavior did not appear in the simulations.

Fig. 4b presents the PMF curve for Ca^{2+} binding at the bridging site of C-S-H. Ca^{2+} ions show a strong affinity for this site, with a ΔG_{min} of −12 J/mol at a distance of 1.9 Å and an energy barrier of about 20 kJ/mol. $Eu(OH)_4^-$, however, binds even more strongly and is likely to displace Ca^{2+} from the silanol group at the bridging site. In comparison, the $Ca[Eu(EDTA)]^+$ and $Ca_2[Eu(EDTA)]^{3+}$ complexes have binding strengths closer to those of Ca^{2+}, indicating that competition for the site is likely. Even though the presence of EDTA can potentially complex and remove Ca^{2+} from the sorption sites [61], its concentration in the studied systems is much lower than that of Ca^{2+} and the competition can be considered negligible.

Fig. 5 displays two representative snapshots from PMF simulations, showing the $Eu(EDTA)^-$ and $Ca_2[Eu(EDTA)]^{3+}$ complexes, both at the lowest energy distance window. The blue circle highlights the bridging sorption site. In both cases, inner sphere coordination is confirmed between the deprotonated silanol group and Eu(III).

In the first complex (Fig. 5a) without coordinated Ca^{2+}, there is a higher negative charge density, which attracts to the positively charged surface of C-S-H (due to surface-bound Ca). Consequently, three deprotonated carboxyl groups of EDTA form outer sphere complexes with surface Ca ions (OS-Ca). In contrast, the second complex (Fig. 5b), with two coordinated Ca ions, is restricted from approaching the surface sufficiently close to interact with additional surface Ca, which may be the reason for the observed reduction in sorption strength. Similarly, the sorption behavior of the $Ca[Eu(EDTA)]^+$ closely resembles that of the $Ca_2[Eu(EDTA)]^{3+}$ complex, as the carboxyl groups remain distant from the surface, preventing further coordination with surface-bound Ca ions.

This highlights the impact of the carboxyl groups of the ligand and molecular geometry on the complex sorption behavior. In our previous study, we evaluated the sorption of the Eu(III)/gluconate complex similarly and found no inner sphere coordination of Eu(III) at the bridging site [25]. Unlike EDTA, gluconate contains multiple alcohol groups but only a single carboxyl group.

3.1.2. *Sorption on the defect sorption site*

The defect site is the most common sorption site on the (001) surface of C-S-H with a high Ca/Si ratio. It contains two negatively charged, deprotonated silanol groups from adjacent Si tetrahedra and has a geometry distinct from the bridging site. This site is surrounded by a higher density of surface Ca ions and is located closer to other sorption sites. Eu(III) is sorbed at the defect site through inner sphere coordination with two deprotonated silanol groups ($\Delta G_{min} = -30$ kJ/mol at $d = 1.8$ Å) and has a high barrier for desorption, with an energy difference of around 60 kJ/mol [25]. The free energy of adsorption of the Eu/EDTA complexes is shown in Fig. 6a (Table SI-3 in Supporting Information).

All three PMF curves show a very steep increase in energy (> 100 kJ/mol) at distances between 3 and 4 Å from the defect site. For the $Eu(EDTA)^-$ and $Ca_2[Eu(EDTA)]^{3+}$ complexes the closest energy minima are found at $d = 1.7$ Å and 2.4 Å after the energy barrier. Although inner sphere coordination for Eu/EDTA complexes both with and without Ca is revealed, the energy barrier to approach it is too high, and it makes the inner sphere binding statistically insignificant or even not probable at all. It can be concluded that the Eu/EDTA complexes do not bind directly

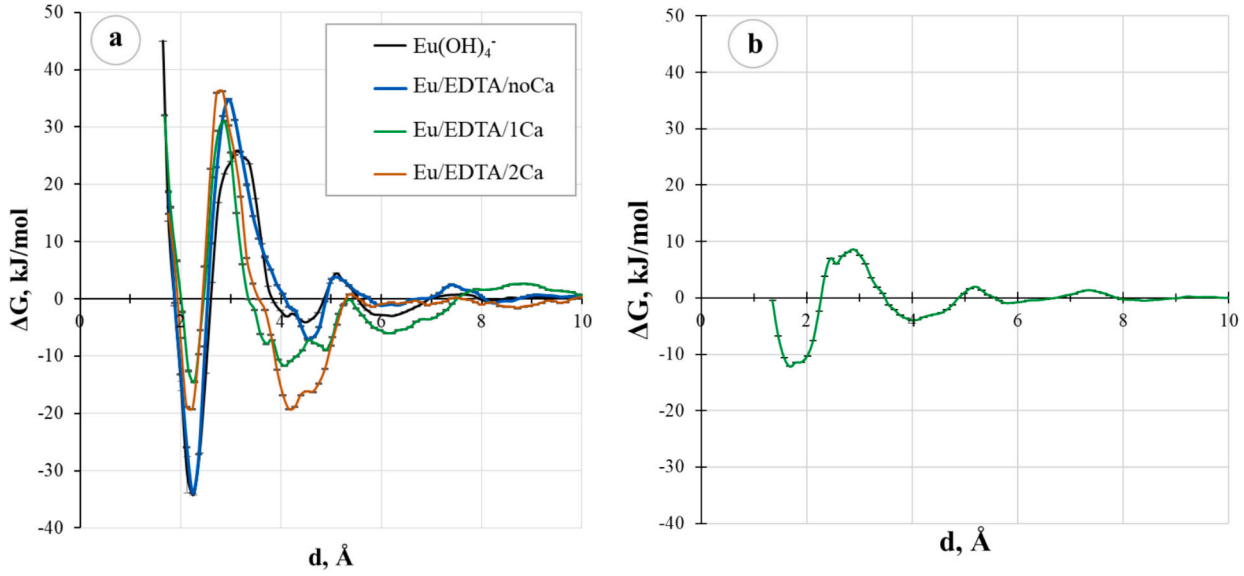

Fig. 4. Potential of mean force curves between (a) the bridging sorption site of C-S-H surface and Eu(III) coordinated with aqueous hydroxyls, EDTA, and varying numbers of Ca^{2+}: $Eu(OH)_4^-$ - Eu(III) hydroxocomplex; Eu/EDTA/noCa – Eu(III) complex with EDTA without Ca^{2+}; Eu/EDTA/1Ca - Eu(III) complex with EDTA with one Ca^{2+}; Eu/EDTA/2Ca – Eu(III) complex with EDTA with two Ca^{2+}; and (b) between the bridging sorption site and Ca^{2+}.

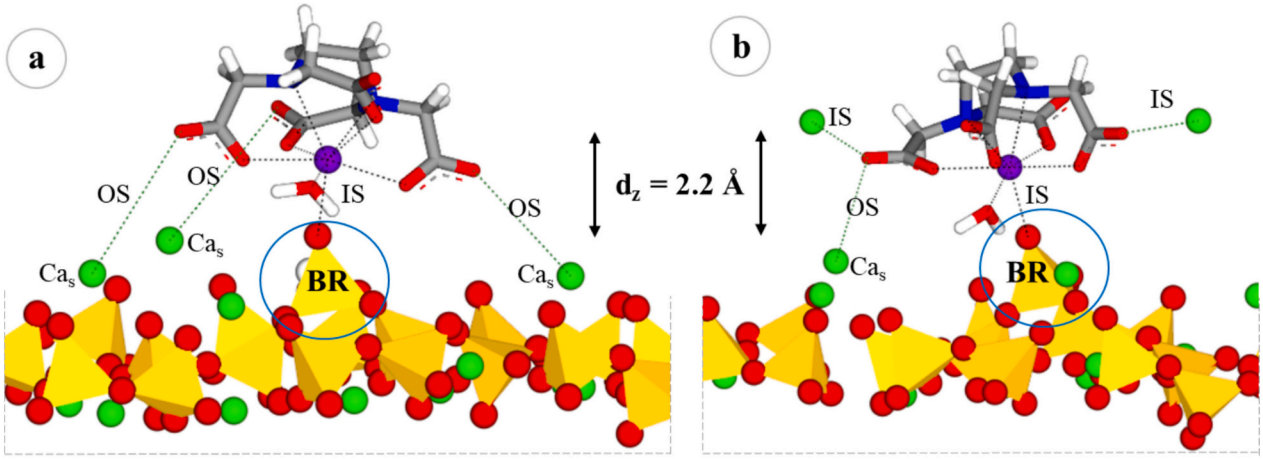

Fig. 5. Simulation snapshots of the Eu/EDTA surface complexation at the bridging sorption site (BR, marked with blue circles): (a) for Eu/EDTA without Ca^{2+} at the PMF window at $d_z = 2.2$ Å; (b) for the Eu/EDTA/2Ca complex at the PMF window at $d_z = 2.2$ Å. Colour scheme: Eu – lilac, O – red, C – grey, H – white, N – blue, Ca – green, Si – yellow. OS – outer sphere, IS – inner sphere, Ca_s – surface Ca. (For interpretation of the references to colour in this figure legend, the reader is referred to the web version of this article.)

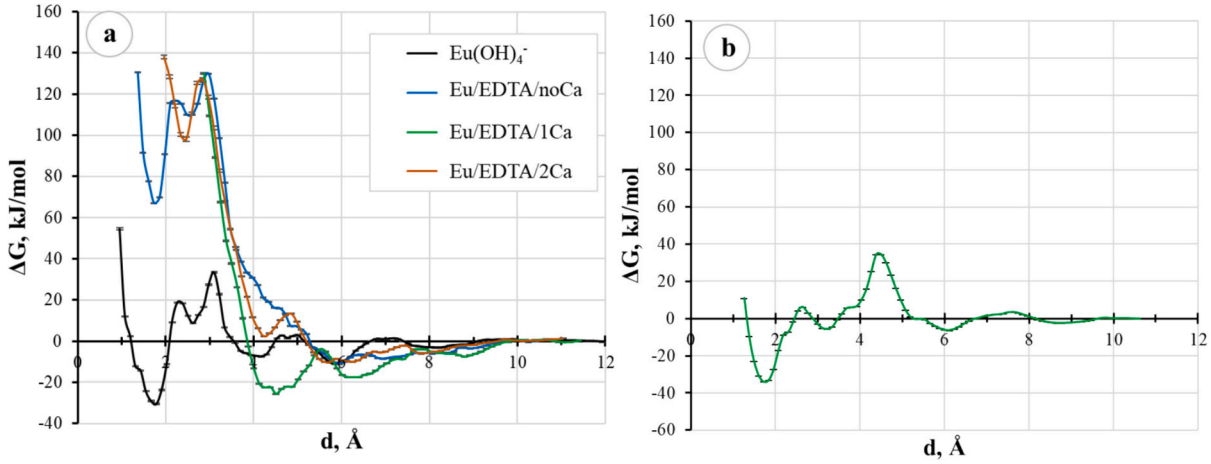

Fig. 6. Potential of mean force curves between (a) the defect sorption site of the C-S-H surface and Eu(III) coordinated with aqueous hydroxyls, EDTA, and varying numbers of Ca^{2+}: $Eu(OH)_4^-$ - Eu(III) hydroxocomplex; Eu/EDTA/noCa – Eu(III) complex with EDTA without Ca^{2+}; Eu/EDTA/1Ca - Eu(III) complex with EDTA with one Ca^{2+}; Eu/EDTA/2Ca – Eu(III) complex with EDTA with two Ca^{2+}; and (b) the defect sorption site and Ca^{2+} (b).

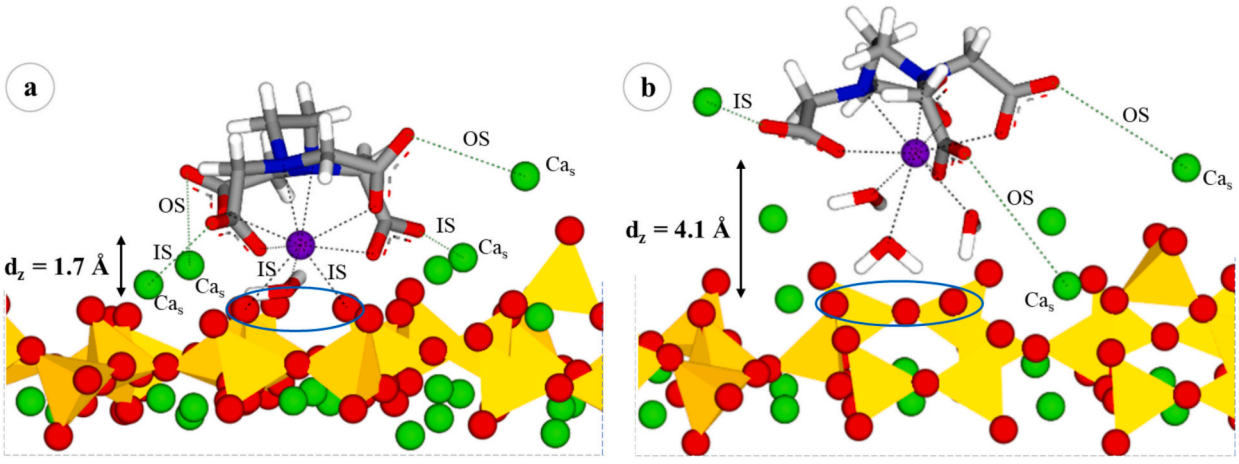

Fig. 7. Simulation snapshots of the Eu/EDTA surface complexation on the defect sorption site of C-S-H (marked with blue ellipses): (a) for the $Eu(EDTA)^-$ complex in the PMF window at $d_z = 1.7$ Å; (b) for the $Ca[Eu(EDTA)]^+$ complex in the PMF window at $d_z = 4.1$ Å. Colour scheme: Eu – lilac, O – red, C – grey, H – white, N – blue, Ca – green, Si – yellow. OS – outer sphere, IS – inner sphere, Ca_s – surface Ca. (For interpretation of the references to colour in this figure legend, the reader is referred to the web version of this article.)

to the deprotonated silanol groups of the defect site and only find favorable coordination as an outer sphere surface complex as in the case of $Ca[Eu(EDTA)]^+$ ($\Delta G_{min} = -20$ kJ/mol at $d = 4.1$ Å, Fig. 7b).

From the PMF curve in Fig. 6b (Table SI-4 in Supporting Information), it can be seen that Ca^{2+} cations are very strongly bound to the defect sorption site: with a main minimum at around 1.9 Å, where Ca coordinates both of the silanol groups of the defect site; a smaller minimum at 2.6 Å, where Ca is connected only to a single silanol; and a high-energy barrier to detach Ca from the site. These Ca^{2+} cations will not be easily substituted by the Eu/EDTA complexes and will not allow the sorption to occur at the defect site.

The inner sphere surface coordination of the $Eu(EDTA)^-$ complex is shown in Fig. 7a, where two of the coordinated water molecules were exchanged for two deprotonated silanol groups of the sorption site. The strong minimum is seen on the PMF curve at d = 1.7 Å. The sorbed complex has inner sphere coordination of carboxyl oxygens with two closest surface Ca and additional outer sphere coordination with two more Ca as seen in the snapshot. The sorption of the complex is controlled by the electrostatic interaction and steric hindrances that form close to the surface. Although the energy gain to form this complex is significant (ΔG = 40 kJ/mol) and shows the complexation that is as strong as in the case of $Eu(OH)_4^-$ sorption (ΔG = 50 kJ/mol), the energy barrier to form this complex is prohibitively high (ΔG = 130 kJ/mol).

3.2. Comparison with experimental data

Here we present a direct comparison of the molecular dynamics results with experimental data reported in Thumm et al. [24] for the same studied system. The uptake of Eu(III) by C–S–H phases in the absence and presence of [EDTA] in $CaCl_2$ and NaCl solutions is shown in Fig. 8 (a) and Fig. 8 (b), respectively. In $CaCl_2$ solutions, Eu(III) sorbs strongly at [EDTA] $< 10^{-3}$ M with a log R_d in the range between 4.5 and 5.5, while at [EDTA] $= 10^{-2}$ M, the retention was significantly decreased to log $R_d \sim 2.8$. In NaCl solutions, C–S–H phases with Ca/Si ≤ 1.1 showed consistently high log R_d values throughout the complete range of EDTA concentrations after 50 days of equilibration (Thumm et al. [24]). For C–S–H phases with Ca/Si ~ 1.4 (characterized by greater concentration of Ca in the aqueous phase), a similar behavior as for $CaCl_2$ systems is observed, i.e., strong sorption at [EDTA] $< 10^{-3}$ M, and a significant decrease in the uptake at higher ligand concentrations (Fig. 8 (a)).

The results in this work align well with these experimental findings. Molecular dynamics simulations suggest that an excess of Ca^{2+} and a relatively high concentration of EDTA stabilize Eu(III) in solution by forming a stable ternary complex (Ca-Eu(III)-EDTA). Moreover, sorption at the bridging site would account for the weaker sorption still observed in the batch sorption experiment (to log $R_d \sim 2.8$ at [EDTA] $= 10^{-2}$ M). In those systems presenting lower Ca concentrations in the aqueous phase (i.e., C–S–H with Ca/Si ≤ 1.1 in NaCl solutions), the binary complex $Eu(EDTA)^-$ prevailing in solution can sorb as inner sphere complex on bridging sorption sites.

This interpretation is further supported by TRLFS data reported in Thumm et al. [24]. Fig. 9 shows Cm(III) TRLFS spectra for C–S–H ~ 1.4 systems in 0.33 M $CaCl_2$ and [EDTA] $= 10^{-2}$ M. The main signal at 603.8 nm corresponds to the ternary Ca–Cm(III)-EDTA complex, and a slight shoulder visible at a wavelength of 607–608 nm was tentatively assigned to quaternary Ca-Cm(III)-OH-EDTA species. Very similar features are obtained for the aqueous phase and C–S–H suspension, thus confirming a weak sorption and that the formation of strong complexes with EDTA and Ca stabilizes Cm(III) in the aqueous phase. Similar

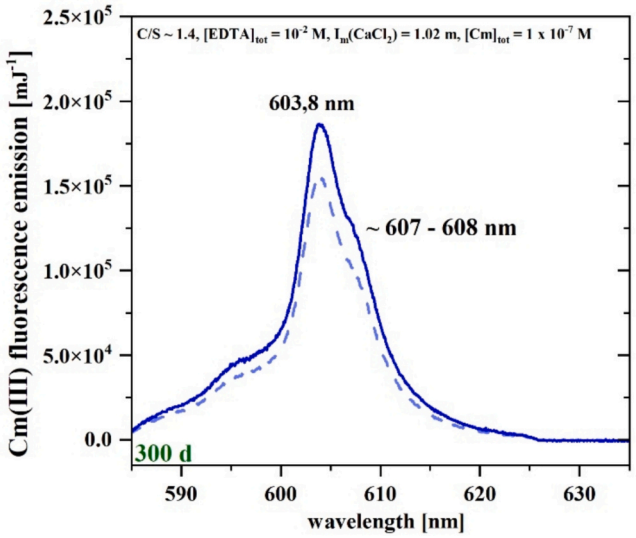

Fig. 9. Fluorescence emission spectra for Cm(III) in the presence of EDTA and C-S-H phases in $CaCl_2$ solution (S/L = 1 g/L; 300 d of contact time; solid line – suspension, dashed line – supernatant) (Thumm et al. [24]).

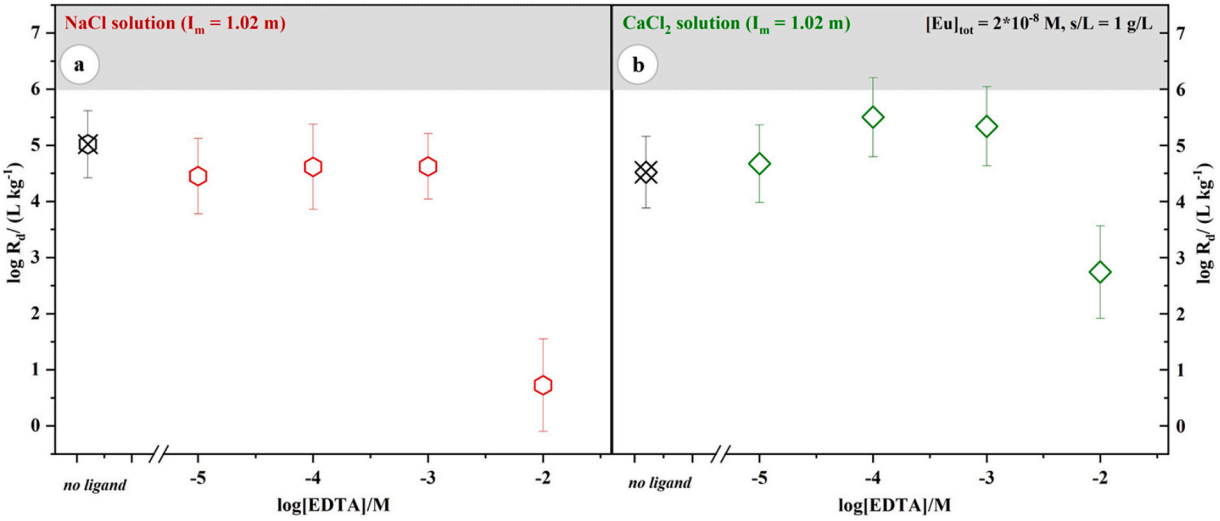

Fig. 8. (a) Distribution coefficients for the sorption of Eu(III) on C-S-H phases (Ca/Si ~ 1.4) in the presence of EDTA in $CaCl_2$ solution at equilibration time of 50 days (S/L = 1 g/L, $[Eu]_{total} = 2{\cdot}10^{-8}$ M) (b) Distribution coefficients for the sorption of Eu(III) on C-S-H phases (Ca/Si ~ 1.4) in the presence of EDTA in $CaCl_2$ solution at equilibration time of 50 days (S/L = 1 g/L, $[Eu]_{total} = 2{\cdot}10^{-8}$ M).

complexation behavior with Pu(III) and Cm(III) has been proposed by DiBlasi et al. [30], based on experimental observations and quantum chemistry calculations.

4. Conclusions

In this study, we investigate the sorption behavior of Eu(III)/EDTA complexes on the calcium silicate hydrate (C-S-H) (001) surface in a $CaCl_2$ solution using molecular dynamics (MD) simulations. The complexation behavior of Eu(III) and EDTA in solution is first examined to identify the most probable ternary Eu/EDTA/Ca complexes, which are subsequently used when analyzing sorption studies. Three configurations were chosen to represent different coordination environments: $Eu(EDTA)^{-}$, $Ca[Eu(EDTA)]^{+}$, and $Ca_2[Eu(EDTA)]^{3+}$.

To quantify the adsorption behavior, potential of mean force (PMF) calculations were conducted to derive the one-dimensional free energy profiles of adsorption for these complexes on two key sorption sites of the C-S-H (001) surface: the bridging site and the defect site. The results demonstrate that Eu(III) forms highly stable complexes with EDTA and Ca^{2+} in solution, significantly reducing its interaction with the C-S-H surface. Specifically, a substantial reduction in sorption is observed at the bridging site, whereas no sorption is detected at the defect site. The presence of Cl^{-} ions shows no noticeable effect, as they remain as background ions at the interface.

Our findings align well with experimental data, suggesting that Eu(III)/EDTA/Ca complexes are stabilized by additional Ca^{2+}, which decreases their affinity for surface adsorption on C-S-H. This work highlights the importance of ternary complex formation in radionuclide transport and retention in cementitious environments, with implications for predicting the behavior of Eu(III) and similar radionuclides in radioactive waste repositories.

CRediT authorship contribution statement

Iuliia Androniuk: Writing – review & editing, Writing – original draft, Visualization, Methodology, Investigation, Formal analysis, Data curation, Conceptualization. **Aline K. Thumm:** Writing – review & editing, Investigation, Conceptualization. **Andrej Skerencak-Frech:** Writing – review & editing, Supervision, Project administration, Conceptualization. **Marcus Altmaier:** Writing – review & editing, Supervision, Project administration, Funding acquisition, Conceptualization. **Xavier Gaona:** Writing – review & editing, Supervision, Project administration, Funding acquisition, Conceptualization.

Declaration of competing interest

The authors declare that they have no known competing financial interests or personal relationships that could have appeared to influence the work reported in this paper.

Acknowledgments

This work was supported by the German collaborative GRAZ II project (Geochemische Radionuklidrückhaltung an Zementalterationsphasen, Teilprojekt 02E11860C), funded by the German Federal Ministry for the Environment, Nature Conservation, Nuclear Safety and Consumer Protection (BMUV). The authors likewise acknowledge support by the state of Baden-Württemberg through bwHPC and the German Research Foundation (DFG) through grant no INST 40/575-1 FUGG (JUSTUS 2 cluster).

Appendix A. Supplementary data

Supplementary data to this article can be found online at https://doi.org/10.1016/j.comptc.2025.115271.

Data availability

Data will be made available on request.

References

[1] F.P. Glasser, Cements in Radioactive Waste Disposal (International Atomic Energy Agency), 2013, p. 30 (ISSN: 1011-4289).
[2] B. Ma, J.L. Provis, D. Wang, G. Kosakowski, The essential role of cement-based materials in a radioactive waste repository, npj Materials Sustain 2 (2024) 21, https://doi.org/10.1038/s44296-024-00025-9.
[3] M. Ochs, D. Mallants, L. Wang, Radionuclide and Metal Sorption on Cement and Concrete, Springer Cham, 2015, p. 201, https://doi.org/10.1007/978-3-319-23651-3.
[4] E. Wieland, Sorption Data Base for the Cementitious near Field of L/ILW and ILW Repositories for Provisional Safety Analyses for SGT-E2 (Nagra Technical Report 14–08), Paul Scherrer Institut, Villigen, Switzerland, 2014.
[5] B.H. Cho, W. Chung, B.H. Nam, Molecular dynamics simulation of calcium-silicate-hydrate for Nano-engineered cement composites – a review, Nanomaterials 10 (11) (2020) 2158, https://doi.org/10.3390/nano10112158.
[6] F.B. De Souza, K. Sagoe-Crentsil, W. Duan, A century of research on calcium silicate hydrate (C–S–H): leaping from structural characterization to nanoengineering, JACerS 105 (5) (2022) 3081–3099, https://doi.org/10.1111/jace.18304.
[7] E. Bonaccorsi, S. Merlino, A.R. Kampf, The crystal structure of Tobermorite 14 Å (Plombierite), a C−S−H phase, J. Am. Ceram. Soc. 88 (2005) 505–512, https://doi.org/10.1111/j.1551-2916.2005.00116.x.
[8] S. Grangeon, A. Fernandez-Martinez, A. Baronnet, N. Marty, A. Poulain, E. Elkaïm, C. Roosz, S. Gaboreau, P. Henocq, F. Claret, Quantitative X-ray pair distribution function analysis of nanocrystalline calcium silicate hydrates: a contribution to the understanding of cement chemistry, J. Appl. Crystallogr. 50 (2017) 14–21, https://doi.org/10.1107/S1600576716017404.
[9] A. Kumar, B.J. Walder, A. Kunhi Mohamed, A. Hofstetter, B. Srinivasan, A. J. Rossini, K. Scrivener, L. Emsley, P. Bowen, The atomic-level structure of cementitious calcium silicate hydrate, J. Phys. Chem. C 121 (2017) 17188–17196, https://doi.org/10.1021/acs.jpcc.7b02439.
[10] A. Kunhi Mohamed, S.C. Parker, P. Bowen, S. Galmarini, An atomistic building block description of C-S-H - towards a realistic C-S-H model, Cem. Concr. Res. 107 (2018) 221–235, https://doi.org/10.1016/j.cemconres.2018.01.007.
[11] L. Fralova, G. Lefevre, B. Made, R. Marsac, E. Thory, R.V.H. Dagnelie, Effect of organic compounds on the retention of radionuclides in clay rocks: mechanisms and specificities of Eu(III), Th(IV), and U(VI), Appl. Geochem. 127 (2021) 104859, https://doi.org/10.1016/j.apgeochem.2020.104859.
[12] M.J. Keith-Roach, The speciation, stability, solubility and biodegradation of organic co-contaminant radionuclide complexes: a review, Sci. Total Environ. 396 (1) (2008) 1–11, https://doi.org/10.1016/j.scitotenv.2008.02.030.
[13] L.R. Canaval, B.M. Rode, The hydration properties of Eu(II) and Eu(III): An *ab initio* quantum mechanical molecular dynamics study, Chem. Phys. Lett. 618 (2015) 78–82, https://doi.org/10.1016/j.cplett.2014.10.060.
[14] A. Chaumont, G. Wipff, Solvation of uranyl(II), europium(III) and europium(II) cations in "basic" room-temperature ionic liquids: a theoretical study, Chem. Eur. J. 10 (16) (2004) 3919–3930, https://doi.org/10.1002/chem.200400207.
[15] S. Chaussedent, A. Monteil, Molecular dynamics simulation of trivalent europium in aqueous solution: a study on the hydration shell structure, J. Chem. Phys. 105 (1996) 6532–6537, https://doi.org/10.1063/1.472499.
[16] C. Clavaguéra, R. Pollet, J.M. Soudan, V. Brenner, J.P. Dognon, Molecular dynamics study of the hydration of lanthanum(III) and europium(III) including many-body effects, J. Phys. Chem. B 109 (16) (2005) 7614–7616, https://doi.org/10.1021/jp051032h.
[17] M. Hirata, P. Guilbaud, M. Dobler, S. Tachimori, Molecular dynamics simulations for the complexation of Ln^{3+} and UO_2^{2+} ions with tridentate ligand diglycolamide (DGA), Phys. Chem. Chem. Phys. 5 (2002) 691–695, https://doi.org/10.1039/b205127n.
[18] Y. An, M.T. Berry, F.C.J.M. Veggel, Aqueous solutions of europium(III) Dipicolinate complexes: estimates of water coordination based on molecular dynamics simulations and excited state decay rate constants, J. Phys. Chem. A 104 (47) (2000) 11243–11247, https://doi.org/10.1021/jp001534p.
[19] G. Benay, R. Schurhammer, G. Wipff, BTP-based ligands and their complexes with Eu3+ at "oil"/water interfaces. A molecular dynamics study, Phys. Chem. Chem. Phys. 12 (2010) 11089–11102, https://doi.org/10.1039/c000772b.
[20] F.C.J.M. Veggel, D.N. Reinhoudt, New, accurate Lennard-Jones parameters for trivalent lanthanide ions, tested on [18]Crown-6, Chem. Eur. J. 5 (1) (1999) 90–95, https://doi.org/10.1002/(SICI)1521-3765(19990104)5:1<90::AID-CHEM90>3.0.CO;2-8.
[21] M. Burešová, J. Kittnerová, B. Drtinová, Comparative study of Eu and U sorption on cementitious materials in the presence of organic substances, J. Radioanal. Nucl. Chem. 332 (2023) 1499–1504, https://doi.org/10.1007/s10967-022-08705-3.
[22] M. Dario, M. Molera, B. Allard, Effect of Organic Ligands on the Sorption of Europium on TiO2 and Cement at High pH, Technical report, SKB TR-04-04, Svensk Kärnbränslehantering AB, Stockholm, Sweden, 2004.
[23] M. Ochs, F. Dolder, Y. Tachi, Decrease of radionuclide sorption in hydrated cement systems by organic ligands: comparative evaluation using experimental data and thermodynamic calculations for ISA/EDTA-actinide-cement systems, Appl. Geochem. 136 (2022) 105161, https://doi.org/10.1016/j.apgeochem.2021.105161.

[24] A.K. Thumm, A. Skerencak-Frech, X. Gaona, M. Altmaier, H. Geckeis, Uptake of Cm (III) and Eu (III) by C–S–H phases under saline conditions in presence of EDTA: A batch sorption and TRLFS study, Appl. Geochem. 170 (2024) 106087, https://doi.org/10.1016/j.apgeochem.2024.106087.
[25] I. Androniuk, R.E. Guidone, M. Altmaier, X. Gaona, Sorption of Eu(III) on C-S-H phases in the presence of gluconate: a molecular dynamics study, Appl. Geochem. (2024) (paper in review).
[26] R.E. Guidone, Impact of Formate, Citrate and Gluconate on the Retention Behavior of Pu(III/IV), cm(III) and Eu(III) by Cement Phases, Doctoral Thesis,, Karlsruhe Institute of Technology, 2023.
[27] A. Tasi, X. Gaona, Th. Rabung, D. Fellhauer, J. Rothe, K. Dardenne, J. Lützenkirchen, M. Grive, E. Colas, J. Bruno, K. Kallstrom, M. Altmaier, H. Geckeis, Plutonium retention in the isosaccharinate – cement system, Appl. Geochem. 126 (2021) 104862, https://doi.org/10.1016/j.apgeochem.2020.104862.
[28] S. Durand, J.P. Dognon, P. Guilbaud, C. Rabbe, G. Wipff, Lanthanide and alkaline-earth complexes of EDTA in water: a molecular dynamics study of structures and binding selectivities, J. Chem. Soc., Perkin Trans. 2 (2000) 705–714, https://doi.org/10.1039/a908879b.
[29] K. Cernochova, J.N. Mathur, G.R. Choppin, Chemical speciation of am, cm and Eu with EDTA at high ionic strength: thermodynamics and laser fluorescence spectroscopy studies, RCA 93 (12) (2005) 733–739, https://doi.org/10.1524/ract.2005.93.12.733.
[30] N.A. DiBlasi, A.G. Tasi, M. Trumm, A. Schnurr, X. Gaona, D. Fellhauer, K. Dardenne, J. Rothe, D.T. Reed, A.E. Hixon, Pu (III) and cm (III) in the presence of EDTA: aqueous speciation, redox behavior, and the impact of ca (II), RSC Adv. 12 (2022) 9478–9493, https://doi.org/10.1039/D1RA09010K.
[31] G.L. Licup, T.J. Summers, J.A. Sobrinho, A. de Bettencourt-Dias, D.C. Cantu, Elucidating the structure of the Eu-EDTA complex in solution at various protonation states, Eur. J. Inorg. Chem. 27 (2024) e202400042, https://doi.org/10.1002/ejic.202400042.
[32] D. Bosbach, B. Luckscheiter, B. Brendebach, M.A. Denecke, N. Finck, High level nuclear waste glass corrosion in synthetic clay pore solution and retention of actinides in secondary phases, J. Nucl. Mater. 385 (2009) 456–460, https://doi.org/10.1016/j.jnucmat.2008.12.044.
[33] J.J. Beaudoin, L. Raki, R. Alizadeh, A 29Si MAS NMR study of modified C–S–H nanostructures, Cem. Concr. Compos. 31 (2009) 585–590, https://doi.org/10.1016/j.cemconcomp.2008.11.004.
[34] X.D. Cong, R.J. Kirkpatrick, Si-29 MAS NMR study of the structure of calcium silicate hydrate, Adv. Cem. Based Mater. 3 (1996) 144–156, https://doi.org/10.1016/S1065-7355(96)90046-2.
[35] C. Roosz, P. Vieillard, P. Blanc, S. Gaboreau, H. Gailhanou, D. Braithwaite, V. Montouillout, R. Denoyel, P. Henocq, B. Made, Thermodynamic properties of C-S-H, C-A-S-H and M-S-H phases: results from direct measurements and predictive modelling, Appl. Geochem. 92 (2018) 140–156, https://doi.org/10.1016/j.apgeochem.2018.03.004.
[36] S.V. Churakov, C. Labbez, L. Pegado, M. Sulpizi, Intrinsic acidity of surface sites in calcium silicate hydrates and its implication to their electrokinetic. Properties, J. Phys. Chem. C 118 (2014) 11752–11762, https://doi.org/10.1021/jp502514a.
[37] R.J. Kirkpatrick, A.G. Kalinichev, X. Hou, L. Struble, Experimental and molecular dynamics modeling studies of interlayer swelling: water incorporation in kanemite and ASR gel, Mater. Struct. 38 (2005) 449–458, https://doi.org/10.1007/BF02482141.
[38] R.J. Kirkpatrick, A.G. Kalinichev, J. Wang, Molecular dynamics modelling of hydrated mineral interlayers and surfaces: structure and dynamics, Mineral. Mag. 69 (2005) 289–308, https://doi.org/10.1180/0026461056930251.
[39] R.T. Cygan, J.-J. Liang, A.G. Kalinichev, Molecular models of hydroxide, Oxyhydroxide, and clay phases and the development of a general force field, J. Phys. Chem. B 108 (2004) 1255–1266, https://doi.org/10.1021/jp0363287.
[40] R.T. Cygan, J.A. Greathouse, A.G. Kalinichev, Advances in Clayff molecular simulation of layered and Nanoporous materials and their aqueous interfaces, J. Phys. Chem. C 125 (2021) 17573–17589, https://doi.org/10.1021/acs.jpcc.1c04600.
[41] A.G. Kalinichev, J.W. Wang, R.J. Kirkpatrick, Molecular dynamics modeling of the structure, dynamics and energetics of mineral-water interfaces: application to cement materials, Cem. Concr. Res. 37 (2007) 337–347, https://doi.org/10.1016/j.cemconres.2006.07.004.
[42] J. Wang, R.M. Wolf, J.W. Caldwell, P.A. Kollman, D.A. Case, Development and testing of a general amber force field, J. Comput. Chem. 25 (9) (2004) 1157–1174, https://doi.org/10.1002/jcc.20035.
[43] H.J.C. Berendsen, J.R. Grigera, T.P. Straatsma, The missing term in effective pair potentials, J. Phys. Chem. A 91 (1987) 6269–6271, https://doi.org/10.1021/j100308a038.
[44] S. Plimpton, Fast parallel algorithms for short-range molecular dynamics, J. Comput. Phys. 117 (1995) 1–19, https://doi.org/10.1006/jcph.1995.1039.
[45] E. Braun, J. Gilmer, H.B. Mayes, D.L. Mobley, J.I. Monroe, S. Prasad, D. M. Zuckerman, Best practices for foundations in molecular simulations [article v1.1], Living J. Comput. Mol. Sci. 1 (5957) (2019), https://doi.org/10.33011/livecoms.1.1.5957.
[46] W. Humphrey, A. Dalke, K. Schulten, VMD: Visual Molecular Dynamics, J. Mol. Graph. 14 (1996) 33–38, https://doi.org/10.1016/0263-7855(96)00018-5.
[47] J. Kastner, Umbrella sampling. Wiley Interdiscip. Rev.: Comput, Mol. Sci. 1 (2011) 932–942, https://doi.org/10.1002/wcms.66.
[48] G. Fiorin, M.L. Klein, J. Henin, Using collective variables to drive molecular dynamics simulations, Mol. Phys. 111 (2013) 3345–3362, https://doi.org/10.1080/00268976.2013.813594.
[49] A. Grossfield, An implementation of WHAM: the weighted histogram analysis method, 2014. Version 2.0.9, http://membrane.urmc.rochester.edu/wordpress/?page_id=126.
[50] A. Grossfield, P.N. Patrone, D.R. Roe, A.J. Schulz, D.W. Siderius, D.M. Zuckerman, Best practices for quantification of uncertainty and sampling quality in molecular simulations [article V1.0], Living. J. Comput. Mol. Sci. 1 (5067) (2018), https://doi.org/10.33011/livecoms.1.1.5067.
[51] J.N. Mathur, P. Thakur, C.J. Dodge, A.J. Francis, G.R. Choppin, Coordination modes in the formation of the ternary am(III), cm(III), and Eu(III) complexes with EDTA and NTA: TRLFS, 13C NMR, EXAFS, and thermodynamics of the complexation, Inorg. Chem. 45 (2006) 8026–8035, https://doi.org/10.1021/ic052166c.
[52] M.B. Comins, C. Shang, R. Polly, A. Skerencak-Frech, M. Altmaier, A.M. Hixon, X. Gaona, Cm(III) speciation in the presence of citrate from neutral to hyperalkaline conditions and the effect of calcium, Chemosphere 364 (2024) 143233, https://doi.org/10.1016/j.chemosphere.2024.143233.
[53] H. Rojo, X. Gaona, T. Rabung, R. Polly, M. Garcia-Gutierrez, T. Missana, M. Altmaier, Complexation of Nd(III)/cm(III) with gluconate in alkaline NaCl and CaCl2 solutions: solubility, TRLFS and DFT studies, Appl. Geochem. 126 (2021) 104864, https://doi.org/10.1016/j.apgeochem.2020.104864.
[54] A. Tasi, X. Gaona, D. Fellhauer, M. Böttle, J. Rothe, K. Dardenne, R. Polly, M. Grive, E. Colas, J. Bruno, Thermodynamic description of the plutonium–α–d–isosaccharinic acid system II: formation of quaternary ca (II)–Pu (IV)–OH–ISA complexes, Appl. Geochem. 98 (2018) 351–366.
[55] J. Tits, E. Wieland, M.H. Bradbury, The effect of isosaccharinic acid and gluconic acid on the retention of Eu(III), am(III) and Th(IV) by calcite, Appl. Geochem. 20 (2005) 2082–2096, https://doi.org/10.1016/j.apgeochem.2005.07.004.
[56] K. Vercammen, M. Glaus, L.R. Loon, Complexation of Th(IV) and Eu(III) by α-isosaccharinic acid under alkaline conditions, Radiochim. Acta 89 (2001) 393–402, https://doi.org/10.1524/ract.2001.89.6.393.
[57] I. Pointeau, B. Piriou, M. Fedoroff, M.-G. Barthes, N. Marmier, F. Fromage, Sorption mechanisms of Eu3+ on CSH phases of hydrated cements, J. Colloid Interface Sci. 236 (2001) 252–259, https://doi.org/10.1006/jcis.2000.7411.
[58] M.L. Schlegel, I. Pointeau, N. Coreau, P.E. Reiller, Mechanism of europium retention by calcium silicate hydrates: An EXAFS study, Environ. Sci. Technol. 38 (2004) 4423–4431, https://doi.org/10.1021/es0498989.
[59] J. Tits, T. Stumpf, T. Rabung, E. Wieland, T. Fanghänel, Uptake of cm(III) and Eu (III) by calcium silicate hydrates: a solution chemistry and time-resolved laser fluorescence spectroscopy study, Environ. Sci. Technol. 37 (2003) 3568–3573, https://doi.org/10.1021/es030020b.
[60] V. Neck, M. Altmaier, T. Rabung, J. Lützenkirchen, T. Fanghänel, Thermodynamics of trivalent actinides andneodymium in NaCl, MgCl2, and CaCl2solutions: solubility, hydrolysis, and ternaryCa–M(III)–OH complexes, Pure Appl. Chem. 81 (9) (2009) 1555–1568, https://doi.org/10.1351/PAC-CON-08-09-05.
[61] E. Maragkou, I. Pashalidis, Investigations on the interaction of EDTA with calcium silicate hydrate and its impact on the U (VI) sorption, Coat 11 (2021) 1037, https://doi.org/10.3390/coatings11091037.